Available online at www.sciencedirect.com
SCIENCE DIRECT
Earth and Planetary Science Letters 243 (2006) 268–281
EPSL
www.elsevier.com/locate/epsl

New Early Cretaceous paleomagnetic data from volcanic and red beds of the eastern Qaidam Block and its implications for tectonics of Central Asia

Zhiming Sun [a,*], Zhenyu Yang [b], Junling Pei [a], Tianshui Yang [a], Xisheng Wang [a]

[a] *Key Laboratory of Crust Deformation and Processes, Institute of Geomechanics, CAGS, Beijing, China*
[b] *Department of Earth Sciences, Nanjing University, Nanjing, China*

Received 23 June 2005; received in revised form 14 November 2005; accepted 16 December 2005
Available online 26 January 2006
Editor: V. Courtillot

Abstract

In order to better understand anomalously low paleomagnetic inclinations in the Cretaceous rocks of central Asia, a combined geochronologic and paleomagnetic investigation has been performed on Cretaceous basalt sequences intercalated with red beds from Zeku area in the eastern Qaidam Block, northeastern Tibetan Plateau. Potassium–argon (K–Ar) dating indicates that the basalt sequences are of Early Cretaceous age (89.9±2.8 to 112.1±2.4 Ma). Isothermal remanent magnetization (IRM), thermal demagnetization of a three-component IRM, and Curie point experiment suggest that magnetite and hematite dominate in red beds, magnetite in basalt flows. Stepwise thermal demagnetization successfully isolated stable characteristic remanent magnetization (ChRM) from 7 lava flows and 12 red beds sites. The ChRMs of red bed and basalt sites pass fold test and likely represent primary remanent magnetization. The tilt-corrected mean direction from red bed sites (basalts plus baked red bed site) is D_s=18.4°, I_s=55.3°, κ_s=69.1, α_{95}=5.5°, N=11 sites (D_s=16.1°, I_s=52.0°, κ_s=42.6, α_{95}=8.6°, N=8), corresponding to a pole at 75.2°N, 182.3°E with A_{95}=7.07° (76.9°N, 194.9°E with A_{95}=10.0°), respectively. The consistent inclination recorded in red beds and basalts implies no significant inclination shallowing caused by deposition compaction in red beds from the studied area. Compared with the Early Cretaceous poles from the North China Block (NCB) or Eurasia, insignificant post-Early Cretaceous northward motion may have occurred between the Qaidam Block and the NCB. On the basis of the existing regional paleomagnetic data, the Qaidam Block has not experienced wholescale vertical axis rotation since the Early Cretaceous with respect to NCB.

Keywords: Qaidam block; Early cretaceous; paleomagnetic; inclination shallowing

1. Introduction

To quantify continental shortening in the central Asia region caused by the India–Eurasia collision since 55 Ma, paleomagnetic studies mainly on red beds have contributed constraints on the paleogeographic position

* Corresponding author. Key Laboratory of Crust Deformation and Processes, Institute of Geomechanics, CAGS, Beijing, 100081 China. Tel.: +86 10 68422365; fax: +86 10 68422326.
E-mail address: sunzm1209@yahoo.com.cn (Z. Sun).

0012-821X/$ - see front matter © 2005 Elsevier B.V. All rights reserved.
doi:10.1016/j.epsl.2005.12.016

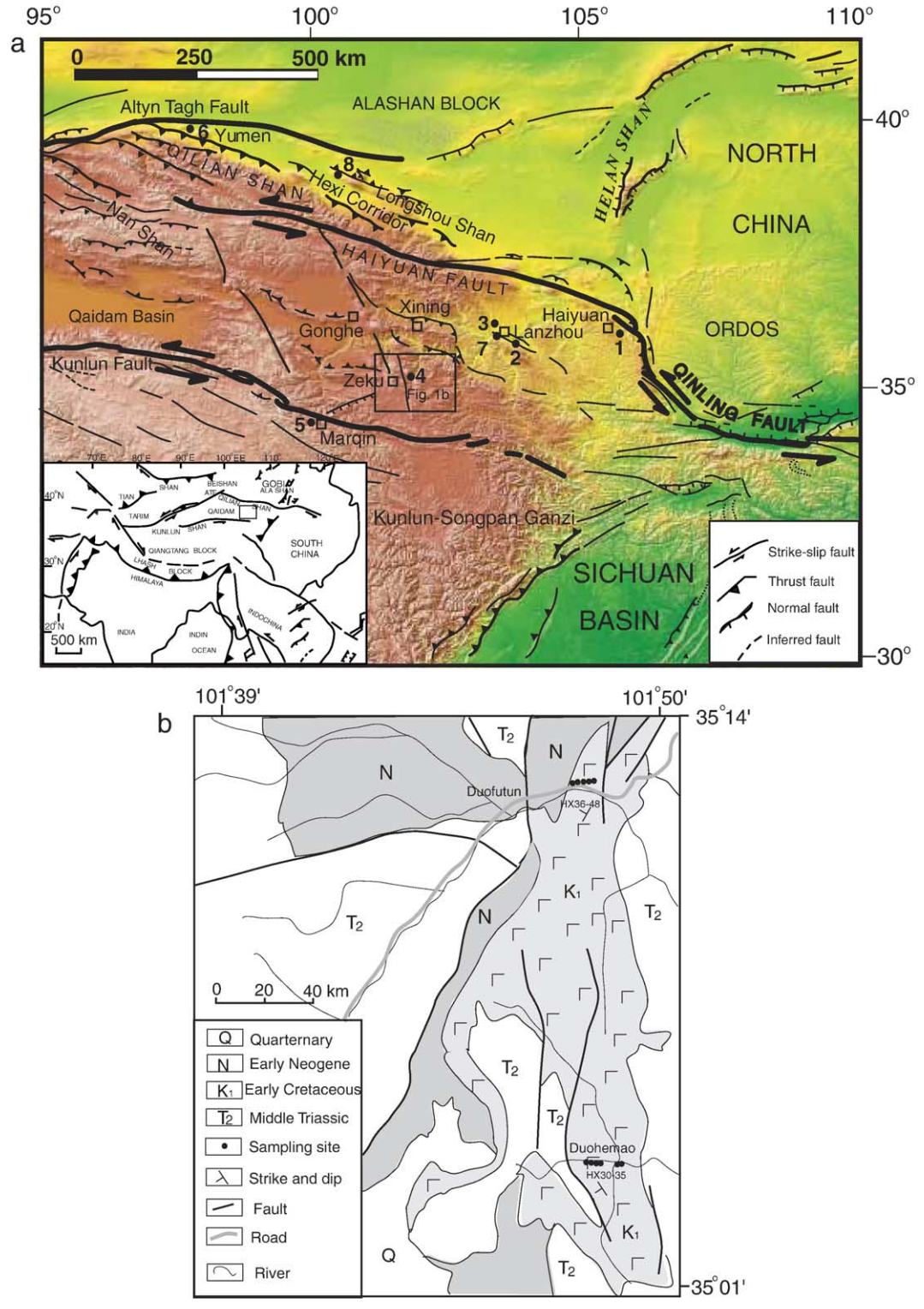

Fig. 1. (a) Simplified topographic map of northeastern Tibetan Plateau with major faults (after [17]). Squares indicate town locations; circles are the paleomagnetic sampling sites. 1, sites of Sun et al. [35]; 2, sites of Yang et al. [19]; 3 and 5, sites of Halim et al. [3]; 4, sites of this study; 6, sites of Chen et al. [4]; 7, sites of Frost et al. [18]; 8, sites of Dupont-Nivet et al. [21]. (b) Geological map of the studied area.

and amount of deformation of major tectonic blocks that comprise the central Asian mosaic (Lhasa, Qiangtang, Kunlun, Tarim, Qaidam, Junggar). Available Cretaceous paleomagnetic data suggests ~1000 km northward movement of the Tarim Block with respect to NCB [1,2]. About 740 km of north–south convergence has taken place between the Qaidam and NCB blocks since at least the Early Cretaceous [3,4]. Such larger continental shortening suggested by paleomagentic studies has not been supported by geological observation and topographic constraints within central Asian mountain ranges. So, several hypotheses have been proposed for these puzzling discrepancies such as poor age control on sediments, syn-sedimentary or compaction-induced inclination shallowing, non-dipolar geomagnetic field geometry, tectonic shortening, tectonic escape, a poorly constrained apparent polar wander path (APWP) for Eurasia, and non-rigidity of the Eurasian plate [5–12] as summarized by Cogne et al. [8] and Gilder et al. [10]. Unfortunately, till to now, none of these causes can reasonably explain the large discrepancies between observed and predicted paleolatitudes in the central Asia during the Cretaceous and Tertiary. This poses a difficult problem in paleogeographic reconstructions of central Asia based on the Cretaceous, especially Tertiary paleomagnetic data of red beds.

Several paleomagnetic studies have been carried out from Cretaceous–Tertiary volcanic rocks in central Asia in order to test whether the paleomagnetic inclination measured in red beds is real [5,13–16]. However, since either no enough volcanic flows are available for sampling to average geomagnetic secular variation to yield a time-averaged pole, or no definite age of volcanic rock can be obtained to constrain the paleomagnetic results, the paleomagnetic poles from the Cretaceous–Tertiary volcanic rocks are disputed recently. For example, Thomas et al. suggested that basalt (~50 Ma) from two sites recorded the similar shallower inclination as red beds [5]. On the contrary, Bazhenov and Mikolaichuk reported that the result of the Paleogene flows (50–74 Ma) from north of Tianshan show no significant inclination shallowing with respect to the synthetic Eurasian APWP [13]. Gilder et al. considered that the Early Cretaceous basalts from Tianshan Mountain likely have steeper inclination than red beds [14].

Previous paleomagnetic results provide important constraints for Cretaceous–Tertiary vertical rotation of northeastern Tibetan plateau under the penetration of India into Asia. Three paleomagnetic studies of Early Cretaceous sediments are available in the northeastern Tibetan plateau (Fig. 1a). Paleomagnetic data from Early Cretaceous rocks in the Hexi corridor and the Xining–Lanzhou basin imply a clockwise rotations of 20–30° within the Nan Shan fold–thrust belt [3,18,19], Chen et al. [20] also inferred that the Qaidam Block experienced >20° clockwise rotation since Early Cretaceous using paleomagentic data from Xining–Lanzhou basin. However, paleomagentic data from Early Cretaceous red beds north of the Hexi corridor indicated no vertical rotations [4,21]. Similarly, no Paleogene and Neogene vertical axis rotations of the Qaidam Basin are suggested by paleomagentic data from the interior of the basin [22,23]. The absence of Cretaceous and Neogene rotation of the Hexi corridor, the Nan Shan fold–thrust belt and the Qaidam Basin disagree with this early interpretation [20]. In this paper, we present paleomagnetic results from Early Cretaceous volcanic rocks intercalated red beds with accurate dating and enough flows in the Zeku area in the eastern Qaidam Block, northeastern Tibetan Plateau (Fig. 1) in order to discuss the inclination shallowing in central Asia, and to constrain Early Cretaceous vertical axis rotations of the Qaidam Block.

2. Geologic setting, sampling and methods

Northeastern Tibetan plateau consists of several structural zones: (a) the Altyn Tagh fault system and associated mountain system, (b) the Qaidam basin, (c) the Kunlun Fault system with its associated mountain belt, and finally, (d) the Qilian Shan range (Fig. 1) [17]. The Qaidam Block is located in the northeastern Tibet Plateau, separated from Kunlun–Songpan Ganzi terrane by Kunlun fault belt to the south, limited by Altyn Tagh fault belt to the northwest and by Qilian Shan to the northeast (Fig. 1).

The sampled locality lies at the eastern margin of the Qaidam Block (Fig. 1). The lower Cretaceous Formation consists of dark-grayish olivine basalt flows intercalated with layers of red sediments with thickness ranging from 4 m to 41 m. Sixteen lava flows were cognized in field with flow thickness between 8 m and 229 m (Fig. 2) [24]. This Formation unconformably overlies Mid-Triassic sandstone and is overlain with angular unconformity by Neogene sandy conglomerates (Fig. 2). The age of this Formation is regarded as Early Cretaceous mainly by regional correlation because of no direct fossil control [24]. Geological evidence and fission tract data indicate that main folding was in the Cenozoic attributed to shortening induced by the Indo-

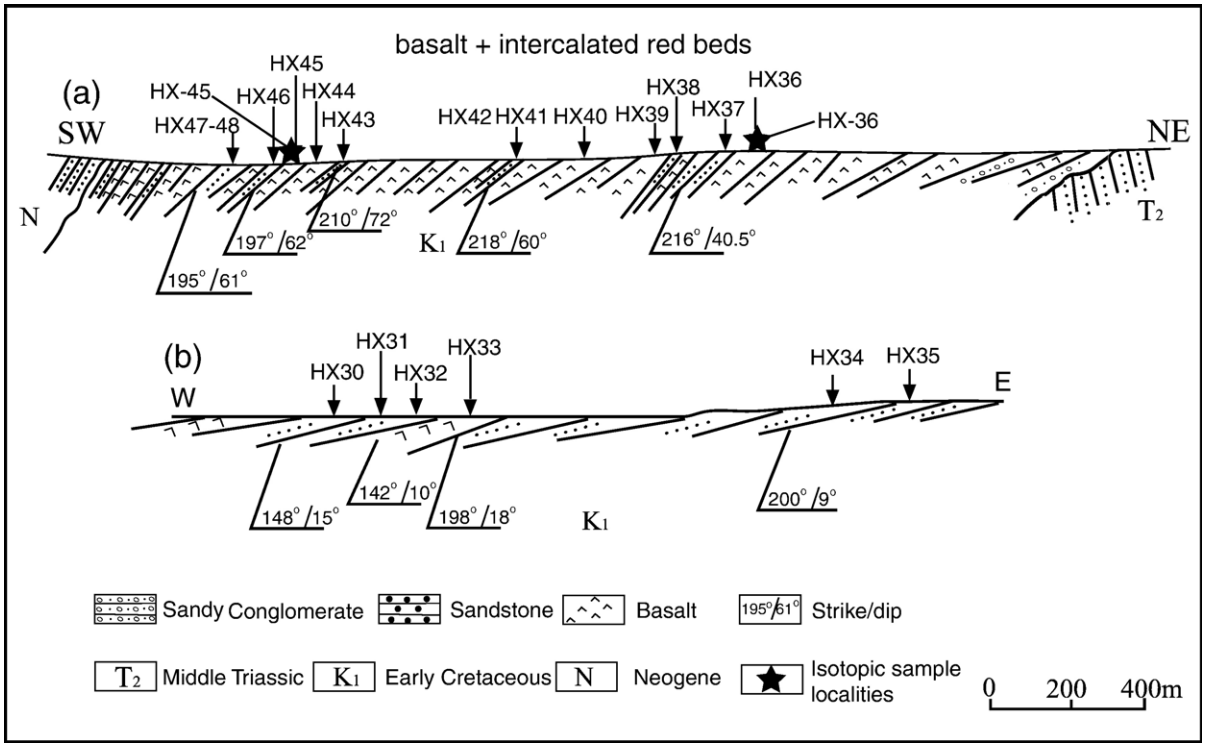

Fig. 2. Measured geological section of the Duofuten (a) and Duohemao (b) section near Zeku county.

Asian collision [25]. The stratigraphy of the Lower Cretaceous Formation is summarized below:

Neogene Formation	
(*unconformity*)	
(5) Olivine basalt and interbeds of red sandstone	~422 m
(4) Olivine basalt intercalated sandstone	~668 m
(3) Olivine basalt and interbeds of red sandstone	~91 m
(2) Large thick olivine basalt	~248 m
(1) Olivine basalt intercalated conlomerate and sandstone	~96 m
(*unconformity*)	
Middle Triassic Formation	

We sampled at two different sections. A simplified structural profile of the Duohemao and Duofuten sections is shown in Fig. 2. Sites HX30-HX35 at 35.06°N/101.8°E were collected in the Duohemao section. Sites HX36-HX48 at 35.2°N/101.8°E in the Duofuten section along a road (Fig. 1b). Altogether we sampled 7 basalt sites and 12 Early Cretaceous red bed sites intercalated in the basalt flows (Fig. 2, Table 2). Each basalt site represents at least one discrete flow. Generally, 10 samples were taken at each site, using a gasoline-powered drill, and were oriented using solar and magnetic compass measurements. In addition, two fresh basaltic samples were collected at the bottom (HX-36) and the top (HX-45) of the studied section respectively for dating of the whole volcanic sequences by a conventional K–Ar method.

All samples from red bed and basalt flows underwent stepwise (17–21 steps) thermal demagnetization in an ASC TD-48 oven with an internal residual field less than 10 nT. Remanent magnetization was measured with a 2G cryogenic magnetometer (red beds) or Schonstedt DSM-2 fluxgate magnetometer (basalts) at the paleomagnetic laboratory of the Institute of Geomechanics, CAGS in Beijing. The magnetometer is located inside a set of large Helmholtz coils that reduced the ambient geomagnetic field to around 300 nT. Remanent components directions were determined by principal component analysis [26]. Site-mean paleomagnetic directions were calculated using Fisherian [27] statistics. A KLY-3S Kappabridge susceptibility system was used to measure the anisotropy of magnetic susceptibility (AMS) of the red bed and basalt samples. In order to characterize the remanence carriers, the acquisition experiments of isothermal remanent magnetization (IRM) were conducted using an ASC Scientific impulse magnetizer model IM-10-30. Thermal demagnetization of a three-component IRM with fields of 0.12 T, 0.4 T and 1.2 T was carried out [28]. Also, thermomagnetic analysis using a Curie balance was performed for selected specimens in both air and vacuum.

3. Experiments and results

3.1. K–Ar dating

The K–Ar dating was conducted in the Key Laboratory of Orogenic Belts and Crustal Evolution, Peking University, China. Fresh rock samples were crushed and sieved to the fraction (60–80 mesh). Olivine crystals that may contain excess argon were removed carefully by using conventional methods to minimize any contribution of argon. Thin nitric acid is used to remove the carbonatization of fresh basalt. Measurements of K content were made by a flame photometer, and Argon gas was analyzed using the isotope dilution technique on a mass spectrometer (RGA10). The detailed measuring processing is outlined in Liu et al. [29]. The K–Ar analytical data and resulting age determination are presented in Table 1. Results indicate that the ages of lower basalt (HX-36) and upper basalt (HX-45) are 112.1± 2.4 Ma , 89.9±2.8 Ma, respectively. This implies that the entire sequence is dated from 112 Ma to 90 Ma. Although K–Ar method can not check existence of extraneous argon or argon loss during weathering, we collected fresh basalt to reduce the probability of such problem. Moreover, thin nitric and conventional methods were used to remove the carbonatization and olivine respectively to minimize their effect on the K–Ar age determination. Thus, we consider that the age of K–Ar dating could be credible. However, further Ar–Ar dating is needed to confirm the K–Ar data.

3.2. Laboratory paleomagnetic analyses

Typical examples of IRM acquisition and thermal decay experiments are shown in Fig. 3. IRM of red bed sample was acquired rapidly up to 0.8 T and not saturated near 2.4 T, indicating that high-coercivity magnetic minerals are dominant (Fig. 3a). The composite IRM indicates that the hard and medium components are unblocked at about 680 °C, while the soft component is mostly unblocked at about 580 °C (Fig. 3b). Curie point experiment shows a marked unblocking temperature in the 680 °C range. The cooling curves are nearly reversible to the heating curves (Fig. 3c). Such thermomagnetic behavior suggests that negligible alteration of the magnetic mineralogy occurs during heating. These imply that red bed sample (HX41-4) contains both magnetite and hematite. In contrast, thermomagnetic curves of basaltic sample are irreversible. Specifically, it is characterized by a high Curie temperature (580 °C) in the heating curve, and distinct lower magnetization in the cooling curve (Fig. 4d and e). The decrease in magnetization seen in the cooling curve probably suggests a phase transformation of magnetite during heating. Together with the thermal demagnetization behavior of basaltic samples, magnetite dominates in most basalt sites.

We measured the AMS of 36 red bed samples and 26 basalt samples. The corrected anisotropy degree (p_j) of the red beds ranges from 1 to 1.04 with only two samples exceeding 1.04 (Fig. 4b). The red beds have a mean anisotropy degree of 1.018. The basalts have a higher mean anisotropy degree of 1.023. For the red beds and basalts, the anisotropy shape factor (T) varies widely, independent of p_j, and is randomly distributed between prolate and oblate forms (Fig. 4a,b). The principal anisotropy directions are dispersed (Fig. 4a). Based on the low degrees of anisotropy and the large scatter in the maximum susceptibility axis directions, we suggest that neither basalts nor red beds have likely experienced significant strain due to compaction or tectonic stress.

Thermal demagnetization isolated a single dominant magnetic component in most basalt samples after removing a recent field or weak viscous magnetization (0–300 °C) (Fig. 5a–f). In general, a high unblocking temperature component (HTC) is often easily isolated between 300 °C and 580 °C or 680 °C. Natural remanent magnetization (NRM) intensity is about 1 A/m in four sites (HX40, HX42, HX44, HX45), and 0.1–0.001 A/m in two sites (HX36, HX39).

The demagnetization behavior of the red beds is similar to that of the basalt samples (Fig. 5g–j). The red bed samples also exhibited a wide range of unblocking temperatures (300–680 °C) except for site HX38 (Fig. 5k). The average NRM intensity in most sites is about 100–1000 times less than basalt samples (0.001–0.0001 A/m vs. 0.1–1.0 A/m). However, the NRM intensities of most of samples from site HX38 (Fig. 5k) were about 10–100

Table 1
Detailed results of K–Ar dating of basaltic rocks from Zeku section, Northeastern Tibet

Sample	K	Weight	$^{40}Ar_{rad}$		^{38}Ar	$^{40}Ar/^{38}Ar$	$^{38}Ar/^{36}Ar$	Age
	(%)	(g)	10^{-10} mol/g	%	10^{-11} mol			(Ma)
HX-36	1.17	0.0247	2.3466	84.03	2.3250	0.2969±0.0004	6056.6±80.1	112.1±2.4
HX-45	0.91	0.0322	1.4544	79.06	2.3203	0.2555±0.0004	5387±47	89.9±2.8

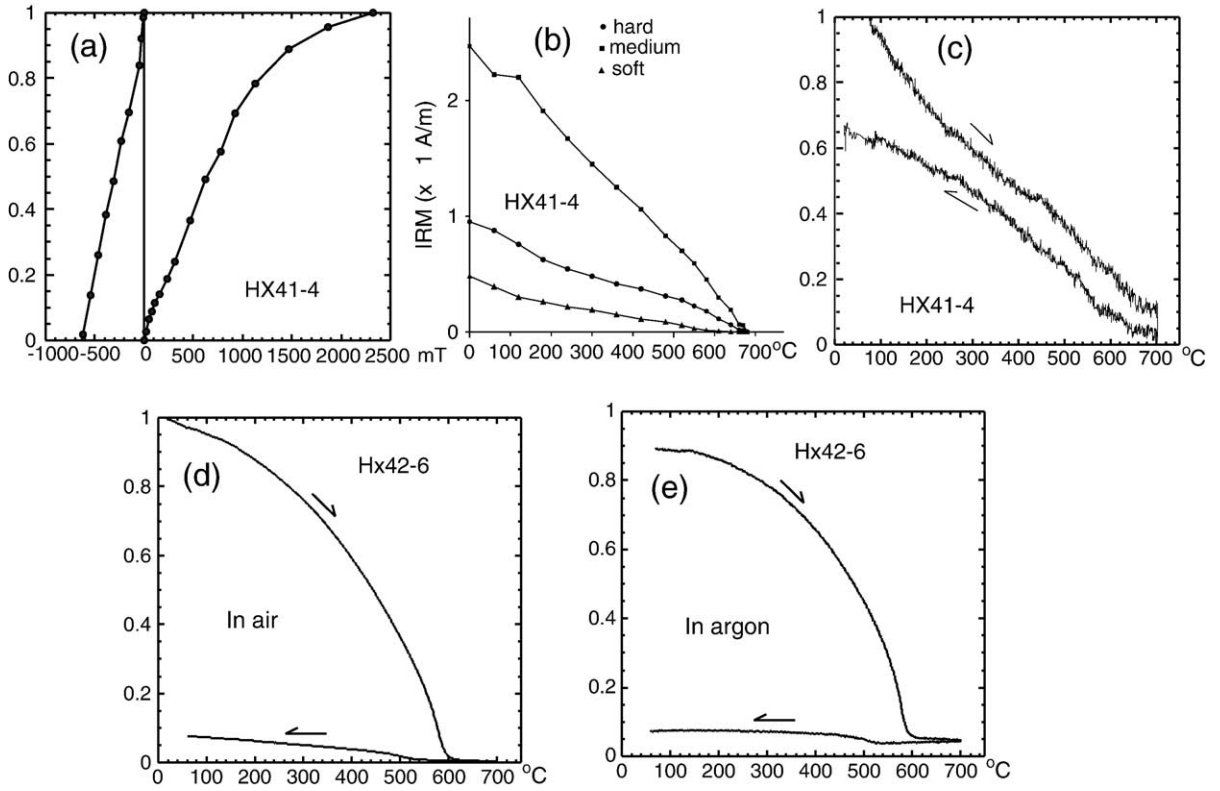

Fig. 3. Normalized isothermal remanent magnetization acquisition curves (a), thermal demagnetization of a three-component IRM (b) of representative red beds, and thermomagnetic curves of magnetization versus temperature (J–T) of representative red beds (c) and basalts (d, e). The soft (<0.12 T), medium (0.12–0.4 T), and hard (0.4–1.2 T) components are shown during thermal demagnetization. Solid line with right (left) arrow corresponds to heating (cooling) curve.

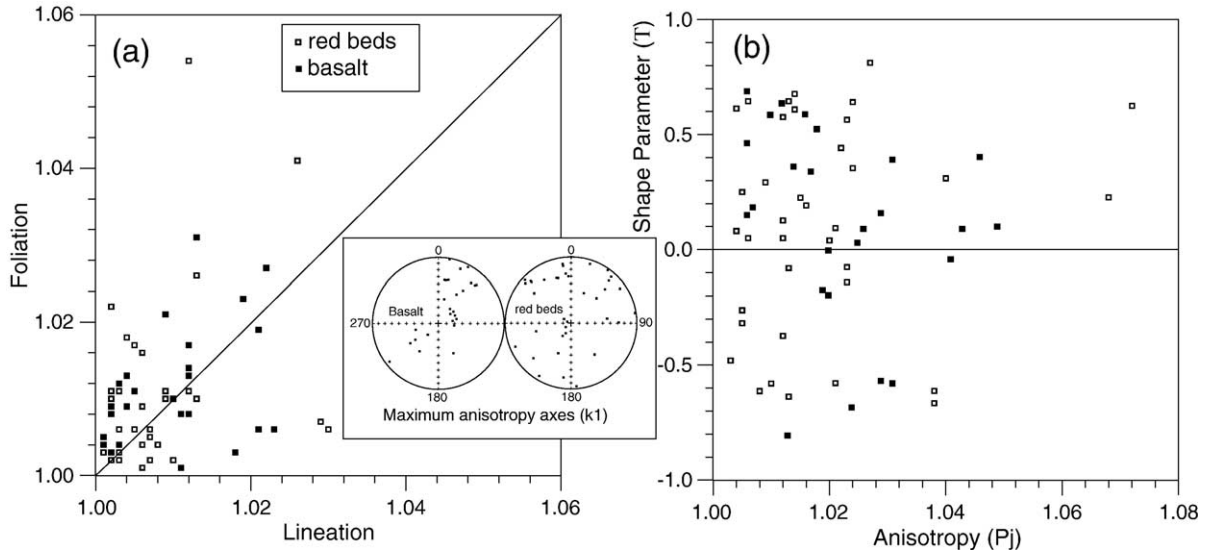

Fig. 4. (a) Anisotropy of magnetic susceptibility data in stratigraphic coordinates from basalts and red beds. Lineation=k_1/k_2, Foliation=k_2/k_3. (b) Plots of shape parameter (T) versus anisotropy degree (P').

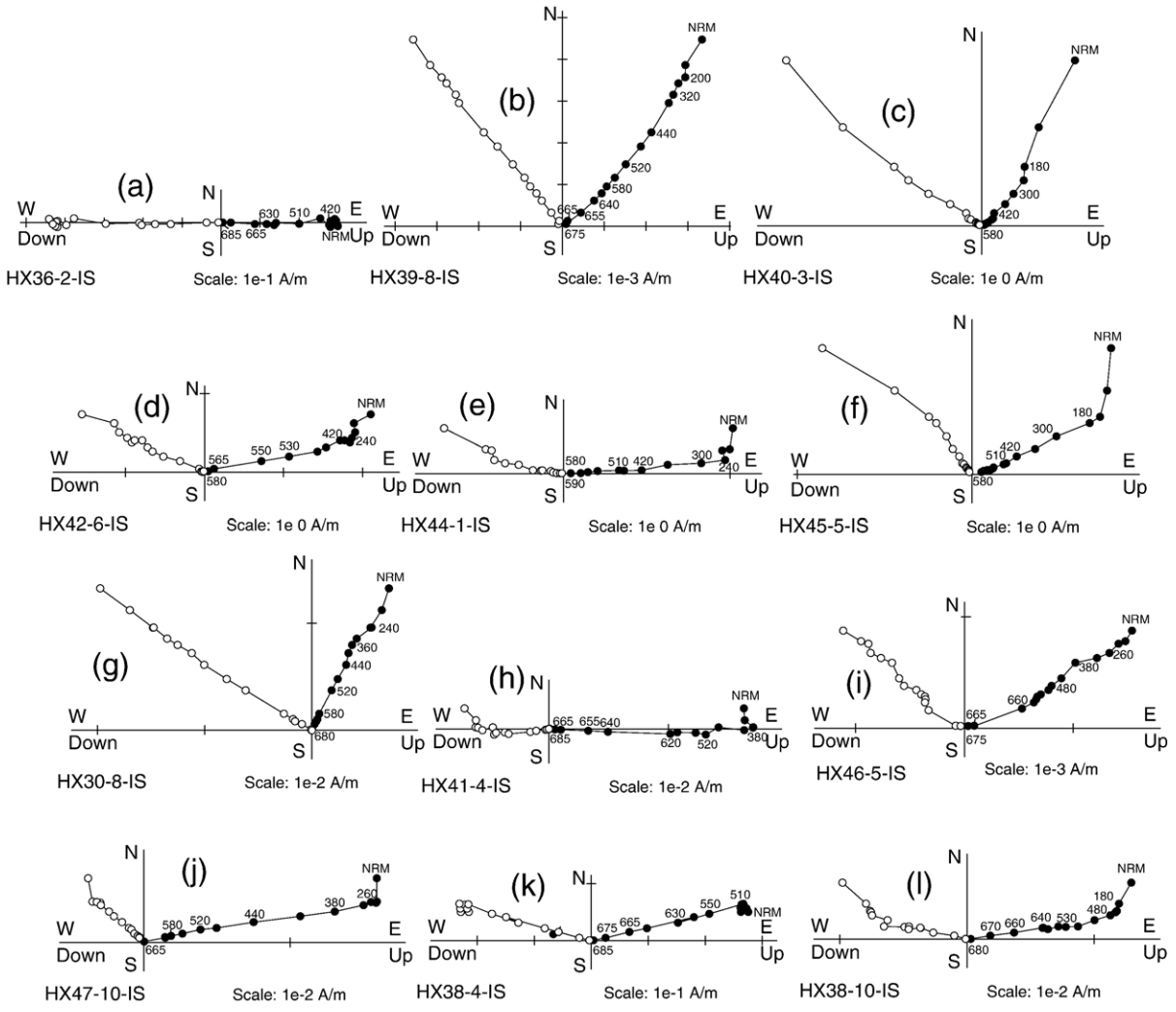

Fig. 5. Orthogonal demagnetization diagrams of representative basaltic rocks and red beds (sample number and corresponding sites listed) in situ coordinates. Demagnetization steps in °C in all plots. NRM is the natural remanent magnetization. a–f: from basaltic rocks , g–j: from red beds, k–l: from baked sites.

times greater than the other samples from the same site (Fig. 5l) and the other Lower Cretaceous red bed sites (Fig. 5g–j), and they exhibited linear demagnetization trend to decay toward the origin in a narrow range of unblocking temperatures (510–685 °C) (Fig. 5k). These demagnetization characteristics, which are similar to that in the baked red beds in Tianshan area reported by Gilder et al. [14], indicate that most of samples from the site HX38 were baked above hematite Curie temperatures, so, their magnetic remanences are thermal, and not depositional or chemical in origin. However, the other red beds sites possess significantly different demagnetization behaviors with relative weaker NRM intensities and wider unblocking temperature than the baked red beds site HX38. These findings indicate that HTC of intercalated red beds samples were not baked above hematite Curie temperatures, and not a remagnetization by heating of the overlain basaltic flows. Thus, we suggest that the directions of the sedimentary samples represent the either depositional or chemical magnetic remanence and not the spot reading of the geomagnetic field. Whereas, some samples had unstable or quite scatter directions on the intrasite level, these samples were omitted in site-mean direction (Table 2).

The site-mean directions are listed in Table 2 and displayed in Fig. 6. The HTC yields a positive fold test at 99% significance level for the basalt plus baked sedimentary site and red beds sites [30]. When all basalt sites plus sedimentary sites, the fold test is also positive. So, we suggest that the remanence is certainly pre-folding and probably primary. As listed in Table 2, only

Table 2
Paleomagnetic results from early Cretaceous red beds and basalts in Zeku area, northeastern Tibet

Site	Slat	Slon	Strike	Dip	*n*/*N*	D_g	I_g	D_s	I_s	κ	α_{95}	Plat	Plon	A_{95}
Red beds														
hx30	35°3.801′	101°49.044′	148	15	8/9	23.7	53.8	6.6	65.2	68.5	6.7	77.0	122	9.8
hx31	35°3.826′	101°49.075′	142	10	7/9	29.1	49.9	23.3	59	70	7.3	71	171	9.4
hx32	35°3.816′	101°49.121′	142	10	9/9	27.9	41.3	23.5	50.4	21.5	11.3	70	196.8	12.4
hx34	35°3.879′	101°49.931′	200	9	9/9	18.8	50.5	8.1	49.7	131.6	4.5	81.7	224.1	4.9
hx35	35°3.879′	101°49.931′	210	11.5	8/9	21.3	54.5	6.5	51.5	232.5	3.6	83.8	219.4	4.0
hx37	35°12.429′	101°49.193′	216	40.5	8/9	80	38.1	37.2	56.3	71.8	6.6	60.1	177.6	8.1
hx38*	35°12.429′	101°49.075′	216	40.5	8/9	81	39.2	36.4	57.5	62.7	7.1	60.8	175.2	8.9
hx41	35°12.372′	101°48.642′	218	60	7/7	73.7	27.5	26.1	43.8	19.7	14	65.6	207.8	13.8
hx43	35°12.38′	101°48.622′	210	72	7/7	81.6	27.7	6.1	54.6	141.2	5.1	85.0	190.9	6.0
hx46	35°12.377′	101°48.596′	197	62	3/9	61.8	25.1	9.6	50.8	141.2	10.4	81.2	213.8	11.5
hx47	35°12.33′	101°48.584′	202	68	3/7	77.9	7.3	40.7	55.1	239.4	16.2	57.1	179	19.4
hx48	35°12.33′	101°48.584′	195	61	9/9	75.6	26.9	11.9	65	42.6	8	75.2	135.2	11.6
Basalt														
hx33	35°3.806′	101°49.232′	198	18	8/9	41.7	48	21.6	52.6	468.5	2.6	72.1	192.0	3.0
hx36	35°12.429′	101°49.193′	216	40.5	8/8	88.2	56.4	4.3	67.2	410.4	2.7	74.9	112.5	4.1
hx39	35°12.429′	101°49.075′	218	60	8/8	52.5	33.5	24.2	35.8	101.1	5.5	63.7	221.2	4.9
hx40	35°12.419′	101°48.993′	201	36	7/7	44	49	0.3	50.2	58.1	8	85.8	278.3	8.8
hx42	35°12.372′	101°48.642′	199	70	7/7	67.5	27.8	359.1	52.5	94.8	6.2	87.8	301.5	7.1
hx44	35°12.38′	101°48.622′	210	72	8/8	78.5	25.8	10.9	52	286.6	3.3	80.6	204.6	3.7
hx45	35°12.38′	101°48.612′	210	72	8/8	69.5	15	25.9	42.8	104.2	5.5	65.4	209.6	5.3
Mean K1 basalt+baked red beds					8	65.7	37.8	–	–	18.4	13.3	–	–	–
						–	–	16.1	52.0	42.6	8.6	76.9	194.9	10.0
Mean k1 red beds					11	56.4	39.4	–	–	10.3	15.0	–	–	–
						–	–	18.4	55.3	69.1	5.5	75.2	182.3	7.0
Mean k1 red beds+basalt					19	60.5	38.8	–	–	12.9	9.7	–	–	–
						–	–	17.4	53.9	56.6	4.5	76.0	187.2	5.4

Slat (Plat): latitude of site (pole); Slon (Plon): longitude of site (pole); *n*/*N*: number of samples used to calculate mean and measured; D_g, I_g, D_s, I_s: declination and inclination in geographic and stratigraphic coordinates, respectively; κ: the best estimate of the precision parameter; α_{95} (A_{95}): the radius that the mean direction (pole) lies within 95% confidence. Unit: degree.
*: Baked red beds.
(1) Fold test for sediments is positive according to McFadden method [30]: critic Xi at 99%=5.37, Xi_2 IS=10.26, Xi_2 TS=0.94.
(2) Fold test for volcanic rocks is positive according to McFadden method [30]: critic Xi at 99%=4.56, Xi_2 IS=5.08, Xi_2 TS=2.21.
(3) Fold test for sediments+volcanic rocks is positive according to McFadden method [30]: critic Xi at 99%=7.11, Xi_2 IS=15.70, Xi_2 TS=2.85.

normal polarity is observed in all basalt and sedimentary sites, this fact is consistent with deposition and magnetization within the Cretaceous Long Normal Superchron with an age between 118 and 83 Ma, and with the basalt K–Ar age of 89.9±2.8 to 112.1±2.4 Ma. The tilt-corrected mean direction from the basalt sites plus baked red bed site HX38 is D_s=16.1°, I_s=52.0°, κ_s=42.6, α_{95}=8.6°, N=8 sites, which corresponds to a pole at 76.9°N, 194.9°E with A_{95}=10.0°. The tilt-corrected mean direction from the red bed sites is D_s=18.4°, I_s=55.3°, κ_s=69.1, α_{95}=5.5°, N=11 sites, the corresponding paleopole lies at 75.2°N, 182.3°E with A_{95}=7.0°.

Since our site-mean directions is based on seven independent basalt flows and one baked red beds site, we are sure that each site is a independent spot reading of the geomagnetic field. We have tested the angular dispersion of the virtual geomagnetic poles (VGP), we obtain a VGP scatter of 12.4°, which fall in the limit (10.1–15.4°) of VGP scatter predicted by McFadden et al. [31] at 35–40° latitude for the 80–110 Ma period. Thus, we suggest that the overall mean direction of the ChRM from basalt flows and baked red beds may have fully averaged out secular variation at the time during flows emplacement and is an accurate estimate of a time-averaged (90–110 Ma) paleomagnetic pole.

4. Discussion

4.1. No wholesale rotation of the Qaidam block or northeastern Tibetan plateau with respect to the NCB and Eurasia since Early Cretaceous

Crustal deformation of the northeastern Tibetan plateau (Qaidam and Qilian Shan, etc.) caused by the

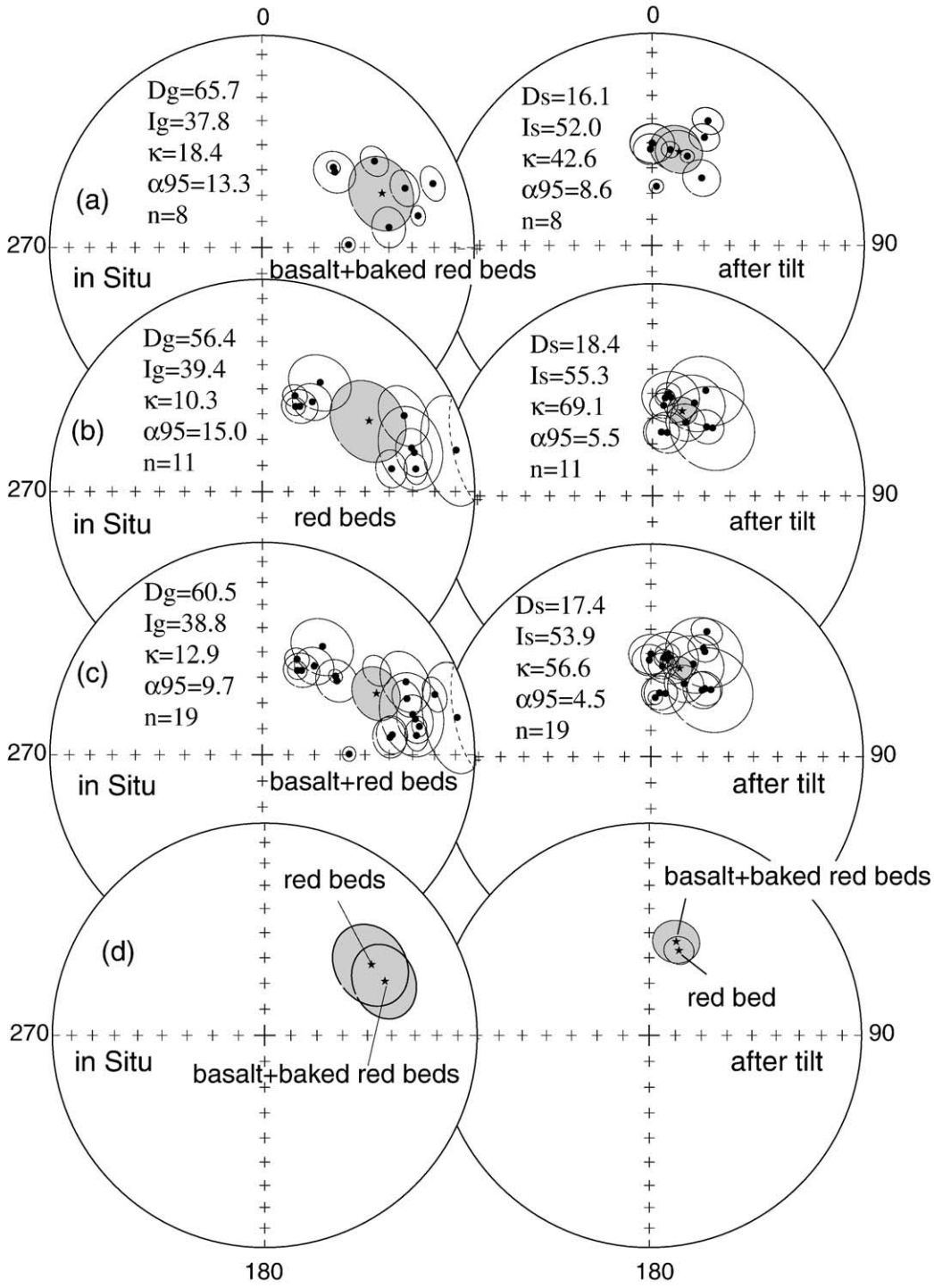

Fig. 6. Equal-area stereographic projections of site-mean directions of the high temperature component in panels a–d (data from Table 2).

India–Asia collision has been the focus of many modeling. In some models [32], clockwise rotation of northeastern Tibetan plateau is generally predicted. Paleomagnetic declinations observed in these regions can be used to test these modeling. Four paleomagnetic studies are available of Early Cretaceous sediments within northeastern Tibet plateau (Fig. 1 and Table 3) [3,18,19,35]. As illustrated in Fig. 7, the

Table 3
Early Cretaceous poles for the northeastern Tibet plateau and adjacent blocks (reference point: 35.2°N, 101.8°E)

Area	Lith.	Lat.	Lon.	N	Plat.	Plon.	A_{95}	Relative to NCB		Relative to Eurasia		Reference
								Latitudinal Difference	Rotation	Latitudinal Difference	Rotation	
Northeastern Tibet plateau												
Haiyuan	Sed.	36.1	105.8	13	78.2	218.0	6.9	0.9±6.0	2.8±7.0	5.0±5.4	0.9±6.4	[35]
Lanzhou	Sed.	35.8	103.9	19	62.2	193.4	3.2	0.2±3.9	17.8±4.6	3.9±3.1	19.6±3.7	[19]
Lanzhou	Sed.	36.2	103.5	10	50.8	195.2	5.5	5.2±5.1	29.4±5.8	9.3±4.5	31.2±5.1	[3]
	Sed.	36.2	103.5	12	56.1	191.6	9.1	1.0±7.4	24.9±8.6	5.2±7.0	26.7±8.1	Recalculated from [3]
Zeku	Bas.+Baked red bed	35.2	101.8	8	76.9	194.9	10.0	−3.4±8.0	0.7±9.5	0.8±7.6	2.4±9.1	This study
	Sed.	35.2	101.8	11	75.2	182.3	7.0	−6.0±6.0	3.2±7.3	−2.0±5.0	4.9±6.8	This study
	Bas.+Baked red bed+Sed.	35.2	101.8	19	76.0	187.2	5.4	−5.0±5.1	2.1±6.1	−0.8±4.4	3.8±5.4	This study
										1.4±6.3[a]	7.0±7.8[a]	This study
Alash	Bas.	41.2	104.0	7	71.1	200.5	2.7	−0.2±3.7	7.3±4.6	4.0±2.8	9.1±3.6	[15]
	Sed.	39.9	97.7	9	75.5	169.9	7.7	−9.1±6.5	3.7±8.6	−4.8±6.0	5.0±8.1	[4]
	Sed.	39.1	100.5	38	82.5	231.7	4.4	−0.3±4.5	−8.7±5.4	3.9±3.8	−7.2±4.6	[21]
Tianshan	Bas.	40.2	75.3	11	64.1	172.1	12.0	−2.7±9.4	19.8±11.1	1.7±9.0	19.2±10.7	[14]
Tarim	Sed.	39.5	75.0	10	70.1	225.8	7.0	7.8±6.0	0.8±6.6	12.1±5.5	1.4±6.0	[2]
	Sed.	41.8	82.0	6	64.6	208.9	9.0	8.5±7.3	9.3±8.2	13.0±6.9	9.1±7.7	[1]
	Sed.	41.6	83.5	10	64	229	11	12.6±8.7	6.5±9.2	18.9±9.5	11.4±10.4	[36]
Mean					66.5	221.0	8.5	8.4±7.0	7.0±7.6	14.8±7.9	11.9±9.1	This study
Kunlun	Sed.	34.5	100.1	13	80.1	281.2	10	4.4±8.0	14.9±8.8	8.7±7.6	13.4±8.4	[3]
NCB	Sed.				76.4	209.5	4.3	–	–	4.2±4.7	1.7±4.4	[33]
SCB	Sed.				78.9	214.9	8.1	−0.1±6.7	3.2±7.8	4.0±6.3	1.5±7.3	[33]
Eurasia (140–80Ma)					79.0	192.6	2.7					[34]
Eurasia (100±10Ma)												

Lith: lithology; Bas: basalt; Sed.: sediments (red bed); Lat. (Lon.): latitude (longitude) of sites; Plat (Plon): latitude (longitude) of pole; A_{95}: the radius that the mean pole lies within 95% confidence. Rotation and latitudinal difference are evaluated by comparison between the observed paleomagnetic result and that expected from the stable NCB and Eurasia (reference point: 35.2°N, 101.8°E). −/+: southward/northward or counterclockwise (clockwise rotation). Unit: degree.

[a] Relative to Eurasia (100±10 Ma).

Early Cretaceous paleopoles from two separate localities of Xining–Lanzhou basin are distinct at 95% confidence limits. However, we noted that the final average excluded two sites (XL4.55 and XL4.56) with higher inclinations and small α_{95} value. The reason to reject them has not been given in the published reference [3]. Indeed, if the result of the two sites were used to calculate the overall mean, the new Early Cretaceous paleopole is not clearly distinct from that in the adjacent locality of Lanzhou basin [19] with 95% confidence level (Fig. 7). After recalculating the mean paleomagnetic data of Xining–Lanzhou basin (Table 2), the Early Cretaceous poles from different regions in the northeastern Tibetan plateau (Zeku, Xining–Lanzhou, Haiyuan) align on a well-defined small circle centered on the reference point (35.2°N, 101.8°E) (Fig. 7). This indicates a constant paleolatitude for the northeastern Tibetan plateau during the Early Cretaceous. However, the Xining–Lanzhou basin shows a large clockwise rotation (17.8°±4.6° to 24.9°±8.6°) with respect to NCB, which could be associated with local smaller block rotation [3,19]. Chen et al. also concluded that the Qaidam Block experienced >20° clockwise rotation based on the paleomagentic data from Neogene sediments in Mahai area within the southern Nan Shan fold–thrust belt [20] and from Lanzhou basin [3,19]. However, paleomagnetic results from Haiyuan area, located to the west of the Xining–Lanzhou basin indicate no vertical axis rotations since Early Cretaceous [35].

In addition, concordant paleomagentic directions were reported in the Zeku area, situated at the internal Qaidam Block (this study). On a more regional scale, the northern part of the Hexi corridor has not experienced vertical axis rotations of Early Cretaceous paleomagnetic directions [4,20]. No significant rotation of

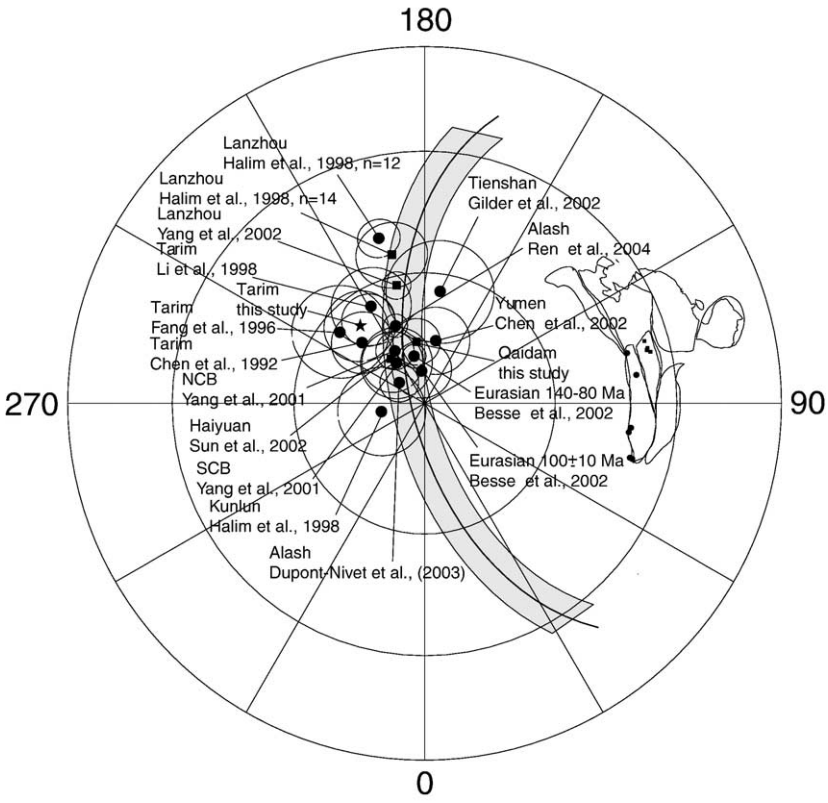

Fig. 7. Comparison of the Early Cretaceous poles between the Qaidam Block and the adjacent blocks. Solid squares indicate the poles from the regions located within the northeastern Tibetan plateau.

the Nan Shan fold–thrust belt has been observed by paleomagnetic results [20]. Similarly, no Paleogene and Neogene vertical axis rotations of the Qaidam Basin are indicated by paleomagnetic results from the interior of the basin [21–23]. These results disagree with this interpretation that the Qaidam Block has experienced >20° clockwise rotation since Early Cretaceous suggested by Chen et al. [4]. This indicates that the Qaidam Block or northeastern Tibetan plateau has not behaved completely rigidly over long distances since the Early Cretaceous because of various mountain range or strike-slip fault systems within the Qaidam Block or northeastern Tibetan plateau, and that heterogeneous deformation may probably exist within the Qaidam Block. Thus, the paleomagnetic data from only one limited area in the Qaidam Block or northeastern Tibetan plateau might not be representative of the wholearea. Combining our analysis of paleomagnetic declination obtained in the above areas, we consider that the Qaidam Block or northeastern Tibetan plateau has not undergone a wholesale regional clockwise rotation accompanied by eastward extrusion of the Tibetan blocks since Early Cretaceous.

4.2. No significant northward displacement of the Qaidam block with respect the adjacent blocks since Early Cretaceous

The mean inclination of the red bed sites (55.3±5.5°) is not different from that of the basalt series plus baked red bed site (52.0±8.6°) within the statistical uncertainty (Fig. 6). This implies that the inclination recorded in red beds in studied section has not suffered from the inclination shallowing due to deposit compaction with respect to that of basalts during the Early Cretaceous. Hence, the mean directions of the basalt series and red beds sites can be combined (D_s=16.9°, I_s=53.9°, κ_s=55.9, α_{95}=4.53°, N=19), the corresponding paleopole lies at 76.0°N, 187.2°E with A_{95}=5.4°. Based on the results of the red beds and basalts, the studied area shows neither significant poleward displacement (1.4±6.3°) nor significant rotation (7.0±7.8°) with respect to the Eurasia [34] since 100±10 Ma (Table 3).

The available Early Cretaceous studies from the adjacent blocks or areas (North China, South China, Tarim, Alashan, Kunlun, Tianshan) are listed in Table

3, the corresponding paleopoles are shown in Fig. 7. The relative north–south movement and rotations with respect to NCB and Eurasia are also given in Table 3.

The small circle that passes over the four poles is fit at a reference point near Zeku area (35.2°N, 101.8°E) with a paleolatitude of 30.8±4.7°. Compared the observed paleolatitude and expected value from the adjacent blocks, the Qaidam Block shows insignificant relative north–south displacement (2.9±8.8°, −3.4±8.0°) with respect to Eurasia, NCB, respectively, within paleomagnetic uncertainties (Table 3). As seen in Fig. 7, The Early Cretaceous poles of the Zeku area (if taken to be the whole Qaidam Block) and the adjacent blocks (Alashan, NCB, SCB) are located within or on the joint intersection of their 95% confidence intervals. This implies that the Qaidam Block was already accreted with these blocks prior to the Early Cretaceous, and that no significant north–south displacement has taken place among above blocks since the Early Cretaceous. Furthermore, Since Triassic time, several continental blocks within northern Tibetan plateau have been accreted to the southern margin of Eurasia by geological observation [37–40]. For example, the Qilian suture between the Qaidam basin and the Alashan massif (block) was formed in the Late Devonian [39], the Kunlun suture between the Kunlun and Qiangtang block is believed to have closed during the Late Triassic [40].

The Early Cretaceous paleopole from the Tarim block implies a large latitudinal motion of 8.0°±5.4° and 12.4°±4.8° with respect to the NCB and Eurasia, respectively (Table 3). Such large amount of N–S convergence referred by the paleomagnetic data exceeds the crustal shortening suggested by geological observation, which may be absorbed in the mountain ranges (Tianshan, Altai). For example, Avouac and Tapponnier estimated that only 125–203 km could have been absorbed for the Tianshan [41]. Dewey et al. gave a 300–400 km shortening in Altai [42]. Furthermore, a few hundred kilometers of convergence in the Tianshan and Altai orogenic ranges could have been neglected because of unobserved geological evidences. As discussed above, The new Early Cretaceous paleomagnetic data of volcanic and red beds from the eastern Qaidam Block, and of sediments from other regions at the northeastern Tibetan Plateau (Table 3) [4,19,21,35] did not support the tectonic escape of central Asia and east Asia along a large left-lateral strike-slip fault during the Tertiary proposed by Halim et al. [3]. Tan et al. suggested that compaction-induced inclination shallowing in Early Cretaceous sediments is the main cause of the large discrepancy of paleomagnetic latitude between the Tarim and NCB or Eurasia [11,12]. However, insignificant inclination shallowing has been found in Early Cretaceous sediments at Yumen area [4], Xining–Lanzhou basin [19], Longshao Shan [21], Haiyuan region [35] and Zeku area, located in the northeastern Tibetan Plateau. These results imply that inclination recorded in the Early Cretaceous sediments at the northeastern Tibetan Plateau is true. Hence, we can fully trust the paleomagnetic constraints on the tectonic movement of the northeastern Tibetan Plateau, at least of the Qaidam Block based on Early Cretaceous red bed studies.

When paleomagnetic results of the Tertiary red beds became available in central Asian, the particularly intriguing is that the inclination shallowing in Tertiary red beds is much stronger than in the Cretaceous red beds. Indeed. As discussed above, northern Tibetan plateau and north of Tibet (Qiangtang, Qaidam, Qilain Shan, Tarim, etc.) have been accreted to Eurasia and suffered no further significant relative northward with respect to it. Tan et al. [11,12] explained that this discrepancy may be caused by inclination shallowing in red beds induced by depositional compaction. As we noted, the compaction-caused inclination shallowing of fine-sand and silt-sized sediments is shown to be negligible by laboratory redeposition and compaction experiments [11]. Most poles of Cretaceous–Tertiary red beds are come from continental quartz-rich sandstone or siltstone rather than clay-rich red beds. Moreover, no difference in inclination values is discerned between the more clay-rich rocks and the coarse-grained layers of Oligo-Miocene sediments at the same section in Subei area, Gansu province [10]. Though some paleomagnetic results from Cretaceous–Tertiary volcanic rocks suggest that the basaltic flows record steeper inclination than red beds [10,13,43]. On the contrary, other volcanic rocks obtain similar shallowing inclination to red beds ([5,15,44,45], this study). Thus, more enough basaltic flows in central Asia are needed to test whether inclination shallowing in Tertiary red beds is so stronger than in Cretaceous red beds. Therefore, we speculate that inclination shallowing in Cretaceous–Tertiary red beds in central Asia can be attributed to non-rigidity of the Eurasian plate since the Cenozoic as suggested by Cogne et al. [8]. When we discuss the Tertiary poles from central Asia, we prefer to use the poles of the SCB or NCB as proxy poles for Siberia, rather than the transferred poles from Europe.

5. Conclusion

We have reported new paleomagnetic results from seven and twelve sites of the Early Cretaceous basalt

flows and red beds respectively collected near Zeku area in the eastern Qaidam Block, northeastern Tibetan Plateau. A high temperature characteristic magnetic component with a single normal polarity is isolated by the stepwise thermal demagnetization. Positive fold test likely suggests a primary magnetization which can be dated at 89.9±2.8∼112.1±2.4 Ma. The consistent inclination recorded in sedimentary and basaltic rocks imply that no significant inclination shallowing has been caused by deposition and/or compaction during the Early Cretaceous in the studied area. On the basis of the previous paleomagentic studies from other localities within northeastern Tibetan plateau, we conclude that the whole Qaidam Block or northeastern Tibetan plateau may have suffered from heterogeneous deformation, and not rotated significantly as a single block with respect to NCB. Compared with the Early Cretaceous poles from the neighboring blocks, the Qaidam Block shows insignificant northward motion with respect to NCB and Alashan within paleomagnetic uncertainties under the effect of the collision of India–Asia. We can fully trust the paleomagnetic constraints on the tectonic movement of the northeastern Tibetan Plateau, at least of the Qaidam Block based on Early Cretaceous red bed studies.

Acknowledgements

This study was supported by NSFC (40102021, 40525013) and by the ministry of Science and Technology (2002CCA05100) and the Key Laboratory of Crust Deformation and Processes, CAGS. We thank Yulin Liu for help in K–Ar dating experiments. We particularly wish to acknowledge Vincent Courtillot (editor), Mikhail Bazhenov, and an anonymous reviewer for very careful and constructive comments. Paleomagnetic data were analyzed using R. Enkin's and J.P. Cogné's [46] computer program packets.

References

[1] Y. Li, Z. Zhang, M. McWilliams, R. Sharps, Y. Zhai, Y. Li, Q. Li, A. Cox, Mesozoic paleomagnetic results of the Tarim craton: tertiary relative motion between China and Siberia, Geophys. Res. Lett. 15 (1988) 217–220.

[2] Y. Chen, J.P. Cogné, V. Courtillot, New paleomagnetic poles from the Tarim Basin, northwestern China, Earth Planet. Sci. Lett. 114 (1992) 17–38.

[3] N. Halim, J.P. Cogne', Y. Chen, R. Atasiei, J. Besse, V. Courtillot, S. Gilder, J. Marcoux, R. Zhao, New Cretaceous and Early Tertiary paleomagnetic results from Xining–Lanzhou basin, Kunlun and Qiangtang blocks, China: implications on the geodynamic evolution of Asia, J. Geophys. Res. 103 (1998) 21,025–21,045.

[4] Y. Chen, H. Wu, V. Courtillot, S. Gilder, Large NS convergence at the northern edge of the Tibetan plateau?: new early cretaceous paleomagnetic data from Hexi Corridor, NW China, Earth Planet. Sci. Lett. 201 (2002) 293–307.

[5] J. Thomas, H. Perroud, P.R. Cobbold, M.L. Bazhenov, V.S. Burtman, A. Chauvin, E. Sadybokasov, A paleomagnetic study of Tertiary formations from the Kyrgyz Tien Shan and its tectonic implications, J. Geophys. Res. 98 (1993) 9571–9589.

[6] M. Westphal, Did a large departure from the geocentric axial dipole hypothesis occur during the Eocene? Evidence from the magnetic polar wander path of Eurasia, Earth Planet. Sci. Lett. 117 (1993) 15–28.

[7] J. Si, R. Van Der Voo, Too-low magnetic inclinations in central Asia: an indication of a long-term Tertiary non-dipole field? Terra Nova 13 (6) (2001) 471–478.

[8] J.P. Cogne', N. Halim, Y. Chen, V. Courtillot, Resolving the problem of shallow magnetizations of Tertiary age in Asia: insights from paleomagnetic data from the Qiangtang, Kunlun, and Qaidam Blocks (Tibet, China), and a new hypothesis, J. Geophys. Res. 104 (1999) 17,715–17,734.

[9] A. Chauvin, R. Perroud, M.L. Bazhenov, Anomalous low Paleomagnetic inclination from Oligocene–lower Miocene red beds of the south–west Tien Shan, Central Asia, Geophys. J. Int. 126 (1996) 303–313.

[10] S. Gilder, Y. Chen, S. Sen, Oligo-Miocene magnetostratigraphy and rock magnetism of the Xishuigou section,Subei (Gansu Province,western China) and implications for shallow inclinations in central Asia, J. Geophys. Res. 106 (B12) (2001) 30505–30525.

[11] X. Tan, K.P. Kenneth, D. Fang, Laboratory depositional and compaction-caused inclination errors carried by haematite and their implications in identifying inclination error of natural remanence in red beds, Geophys. J. Int. 151 (2002) 475–486.

[12] X. Tan, K.P. Kodama, H. Chen, D. Fang, D. Sun, Y. Li, Paleomagnetism and magnetic anisotropy of Cretaceous red beds from the Tarim Basin, northwest China: evidence for a rock magnetic cause of anomalously shallow paleomagnetic inclinations from central Asia, J. Geophys. Res. 108 (B2) (2003) 2107, doi:10.1029/2001JB001608.

[13] M.L. Bazhenov, A.V Mikolaichuk, Paleomagnetism of Paleogene basalts from the Tien Shan, Kyrgyzstan: rigid Eurasia and dipole geomagnetic field, Earth Planet. Sci. Lett. 195 (2002) 155–166.

[14] S. Gilder, Y. Chen, J.P. Cogne, X. Tan, V. Courtillot, D. Sun, Y. Li, Paleomagnetism of Upper Jurassic to Lower Cretaceous volcanic and sedimentary rocks from the western Tarim Basin and implications for inclination shallowing and absolute dating of the M-0 (ISEA?) chron, Earth Planet. Sci. Lett. 206 (2003) 587–600.

[15] S. Ren, R. Zhu, B. Huang, F. Zhang, H. Wang, Paleomagnetic study on orogenic belt: an example from Early Cretaceous volcanic rocks, Inner Mongolia, China, Sci. China 47 (12) (2004) 1127–1133.

[16] Y. Wang, B. Huang, R. Zhu, T. Liu, Paleomagnetic result of the Cenozoic volcanic rocks from the Tuoyun Basin, southwest Tien Shan of China and its tectonic implications, China, Sci. Bull. 49 (12) (2004) 1288–1295.

[17] P. Tapponnier, Z.Q. Xu, F. Roger, B. Meyer, N. Arnaud, G. Wittlinger, J.S. Yang, Oblique stepwise rise and growth of the Tibet plateau, Science 294 (2001) 1671–1677.

[18] G.M. Frost, R.S. Coe, Z. Meng, Y. Peng, Y. Chen, V. Courtillot, G. Peltzer, P. Tapponnier, J.-Ph. Avouac, Preliminary Early

Cretaceous paleomagnetic results from the Gansu Corridor, China, Earth Planet. Sci. Lett. 129 (1995) 217–232.
[19] T. Yang, Z. Yang, Z. Sun, A. Li, New Early Cretaceous paleomagnetic results from the Qilian orogenic belt and its tectonic implications, Sci. China 45 (2002) 565–575.
[20] Y. Chen, S. Gilder, N. Halim, J. Cogné, V. Courtillot, New paleomagnetic constraints on central Asian kinematics: displacement along the Altyn Tagh fault and rotation of the Qaidam Basin, Tectonics 21 (5) (2002) 1042–1061.
[21] G. Dupont-Nivet, R.F. Butler, A. Yin, X. Chen, Paleomagnetism indicates no Neogene vertical rotations of the northeastern Tibetan Plateau, J. Geophys. Res. 108 (2003) 2386, doi:10.1029/2003JB002399.
[22] G. Dupont-Nivet, R.F. Butler, A. Yin, X. Chen, Paleomagnetism indicates no Neogene rotation of the Qaidam Basin in North Tibet during Indo-Asian Collision, Geology 30 (3) (2002) 263–266.
[23] Z. Sun, Z. Yang, J. Pei, X. Ge, X. Wang, T. Yang, W. Li, S. Yuan, Magnetostratigraphy of Paleogene sediments from northern Qaidam Basin, China: implications for tectonic uplift and block rotation in northern Tibetan plateau, Earth Planet. Sci. Lett. 237 (2005), 635–646.
[24] Qinghai Bureau of Geology and Mineral Resources (QBGMR), Regional Geology of the Qinghai Province, Geol. Publ. House, Beijing, 1991 662 pp.
[25] B.K. Horton, G. Dupont-Nivet, J. Zhou, G.L. Waanders, R.F. Butler, J. Wang, Mesozoic–Cenozoic evolution of the Xining–Minhe and Dangchang basins, northeastern Tibetan plateau: magnetostratigraphic and biostratigraphic results, J. Geophys. Res. 109 (2004) B04402, doi:10.1029/2003JB002913.
[26] J.L. Kirschvink, The least-squares line and plane and analysis of paleomagnetic data, Geophys. J. R. Astron. Soc. 62 (1980) 699–718.
[27] R.A. Fisher, Dispersion on a sphere, Proc. R. Soc London, Ser. A 217 (1953) 295–305.
[28] W. Lowrie, Indentification of ferromagnetic minerals in a rock by coercivity and unblocking temperature properties, Geophys. Res. Lett. 17 (1990) 159–162.
[29] Y. Liu, X. Jin, Y. Lei, G. Miao, B. Huang, Preprocessing of volcanic rocks and its influence to age of K–Ar dating, Acta Sci. Nat. Univ. 40 (2004) 189–192.
[30] P.L. McFadden, A new fold test for palaeomagnetic studies, Geophys. J. Int. 103 (1990) 163–169.
[31] P.L. McFadden, R.T. Merrill, M.W. McElhinny, S. Lee, Reversals of the Earth's magnetic field and temporal variations of the dynamo families, J. Geophys. Res. 96 (1991) 3923–3933.
[32] P.C. Engl, G.A. Houseman, Finite strain calculations of continental deformation: 2. Comparison with the India–Asia collision, J. Geophys. Res. 91 (1986) 3664–3676.
[33] Z. Yang, J. Besse, New Mesozoic apparent polar wander path for South China: tectonic consequence, J. Geophys. Res. 106 (2001) 8493–8520.
[34] J. Besse, V. Courtillot, Apparent and true polar wander and the geometry of the geomagnetic field in the last 200 million years, J. Geophys. Res. 107 (B11) (2002) 101029–101060.
[35] Z. Sun, Z. Yang, T. Yang, A. Lin, New Early Cretaceous paleomagnetic results from the Haiyuan area and its tectonic implications, Chin. J. Geophys. 44 (5) (2001) 675–683.
[36] D. Fang, G. Jin, L. Jiang, P. Wang, Z. Wang, Paleozoic paleomagnetic results and the tectonic significance of Tarim plate, Chin. J. Geophys. 39 (1996) 522–532.
[37] Y. Chen, Outline of Chinese Regional Geology, Geologic Publishing House, Beijing, 1994, p. 517.
[38] L. Xia, Z. Xia, X. Xu, Origin of the Oceanic Island Arc System in the Northern Qilian Shan, Geologic Publishing House, Beijing, 1996, p. 153.
[39] Z. Xu, J. Yang, M. Jiang, H. Li, Continental subduction and uplifting of the orogenic belts at the margin of the Qinghai–Tibet plateau, Earth Sci. Front. 6 (1996) 139–151.
[40] C. Chang, N. Chen, M.P. Coward, W. Deng, et al., Preliminary conclusions of the Royal Society/Academia Sinica 1985 Geotraverse of Tibet (24 other authors), Nature 323 (1986) 501–507.
[41] J.P. Avouac, P. Tapponnier, Kinematic model of active deformation in central Asia, Geophys. Res. Lett. 20 (1993) 895–898.
[42] J.F. Dewey, S. Cande, W.C. Pitman, Tectonic evolution of the India–Eurasia collision zone, Eclogae Geol. Helv. 82 (1989) 717–734.
[43] B. Huang, D.A. Piper, Y. Wang, H. He, R. Zhu, Paleomagnetic and geochronological constraints on the post-collisional northward convergence of the southwest Tian Shan, NW China, Tectonophysics 409 (2005) 107–124.
[44] F. Hankard, J.P. Cogné, V. Kravchinsky, A new Late Cretaceous paleomagnetic pole for the west of Amuria block (Khurmen Uul, Mongolia), Earth Planet. Sci. Lett. 236 (2005) 359–373.
[45] V. Bragin, V. Reutsky, K. Litasov, V. Malkovets, A. Travin, D. Mitrokhin, Paleomagnetism and Ar40/39Ar-dating of late Mesozoic volcanic pipes of Minusinsk depression (Russia), Phys. Chem. Earth 24 (1999) 545–549.
[46] J.P. Cogné, PaleoMac: a Macintosh™ application for treating paleomagnetic data and making plate reconstructions, Geochem. Geophys. Geosyst. 4 (1) (2003) 1007, doi:10.1029/2001GC000227.